Basics of electron beam-plasma interactions; experiment and simulation

Rod Boswell

SP3
http://sp3.anu.edu.au
Space Plasma, Power & Propulsion

Space Plasma Power and Propulsion
Research School of Physics and Engineering
The Australian National University

SP3's activities: summary

SP3 undertakes research into
low temperature plasmas and their applications.
Plasma thrusters for nano-sats
PIC simulations and plasma modeling,
plasma processing of surfaces,
atmospheric pressure plasmas for medicine
space physics and thermodynamics

INDUSTRY

EADS-ASTRIUM electric propulsion
Lockheed/Martin electric propulsion
LAM RESEARCH microelectronics
OREGON PHYSICS focused ion beams from Ar, Xe plasma source not liquid metals
SLInnovation, turnkey Ion Routers
Airity/CCS DC/DC conversion and rf generation

Interaction of electron beams with plasmas

If a charged particle passes through a medium with a velocity greater than the phase velocity, then waves are emitted (Heavyside, Čerenkov)

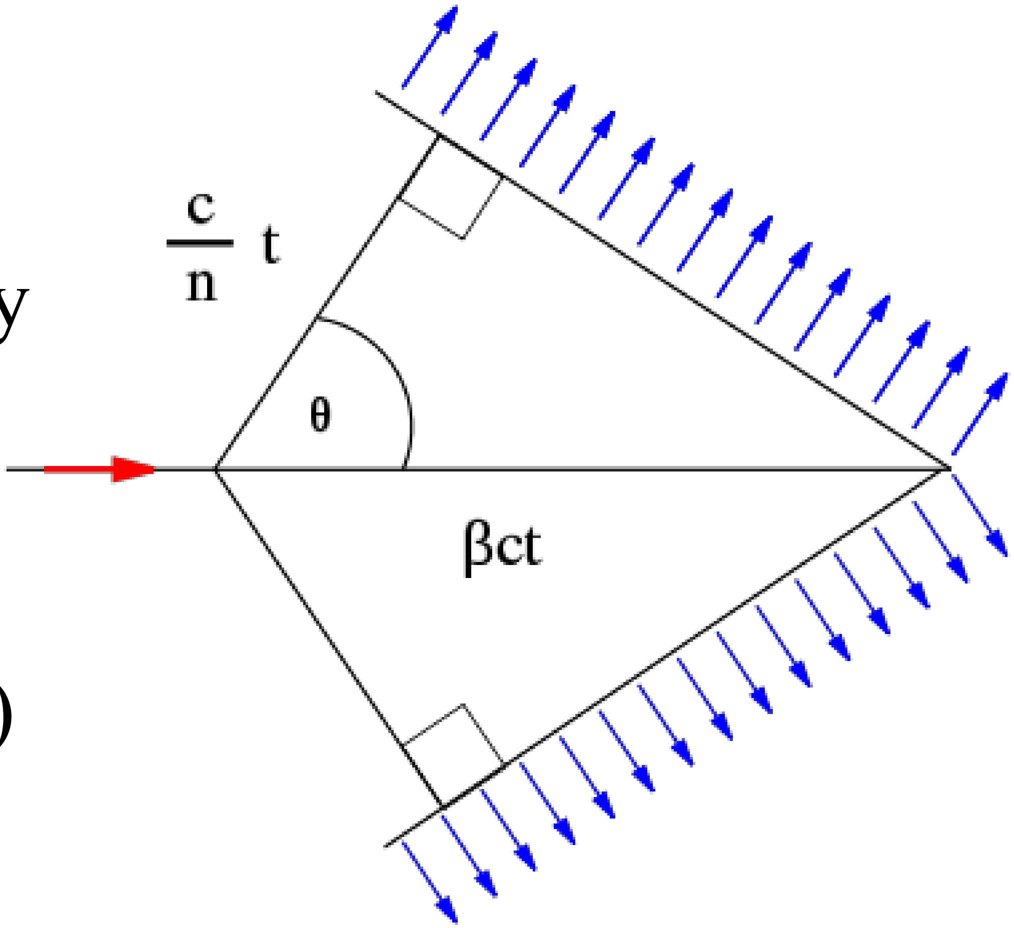

Boats moving faster than surface water waves create a similar wake

Electron beams interact with plasmas in a similar manner, the instability is convective rather than absolute in that it grows along the direction of the beam velocity rather than growing everywhere in time. (from Briggs)

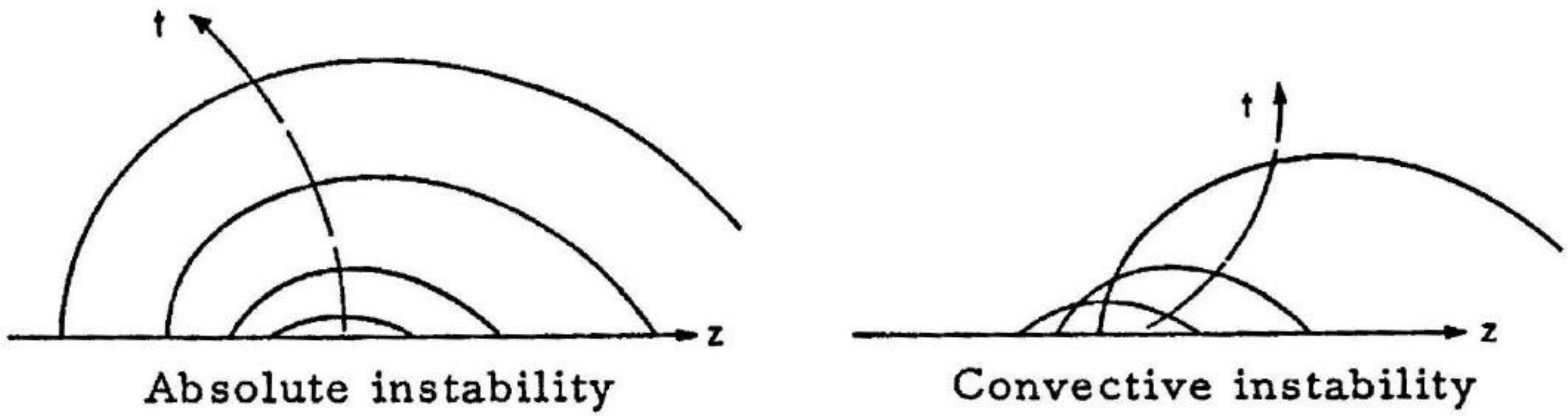

Figure 2.1. Evolution of pulse disturbance in an unstable system.

An unmagnetized plasma supports three natural modes of oscillation (waves)

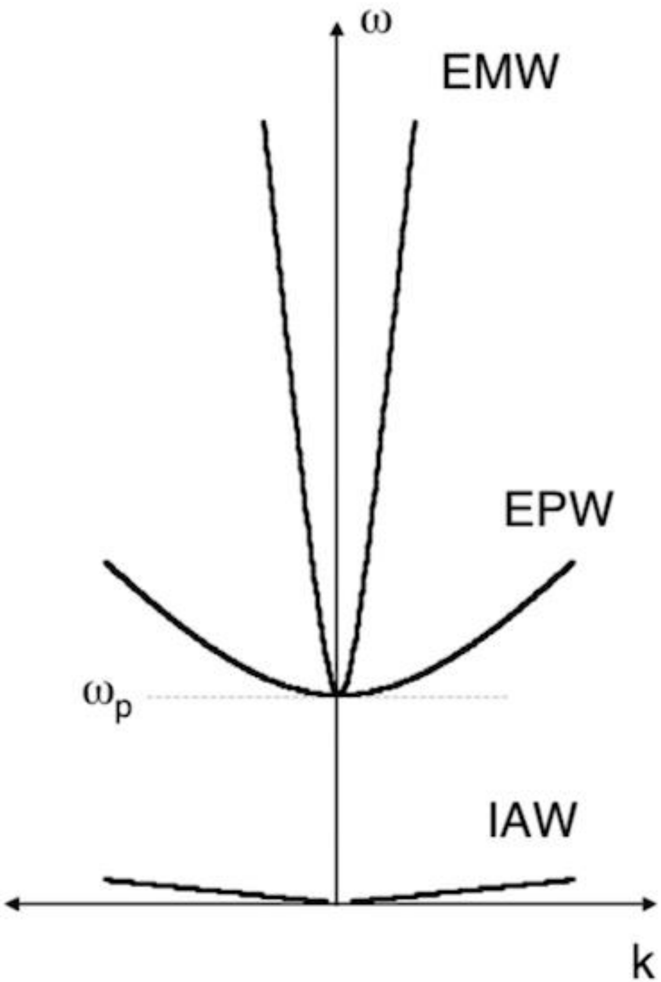

EMW

$$\omega_0^2 = \omega_p^2 + k_0^2 c^2$$

EPW or Langmuir

$$\omega_{epw}^2 \approx \omega_p^2 + 3k_{epw}^2 v_e^2 \approx \omega_p^2\left(1 + 3k_{epw}^2 \lambda_D^2\right)$$

IAW

$$\omega_{iaw} \approx c_s k_{iaw} + \vec{k}_{iaw} \cdot \vec{v}$$

$$\omega_p = \left(4\pi n e^2 / m_e\right)^{1/2}, \; v_e = \left(k_B T_e / m_e\right)^{1/2}, \; \lambda_D = v_e / \omega_p$$

$$c_s \approx \left(Z k_B T_e / M_i\right)^{1/2}$$

How does a 3-wave parametric instability grow in a plasma?

Step 1

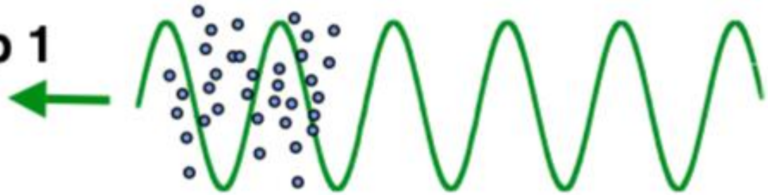

Laser light propagates through the plasma

Step 2

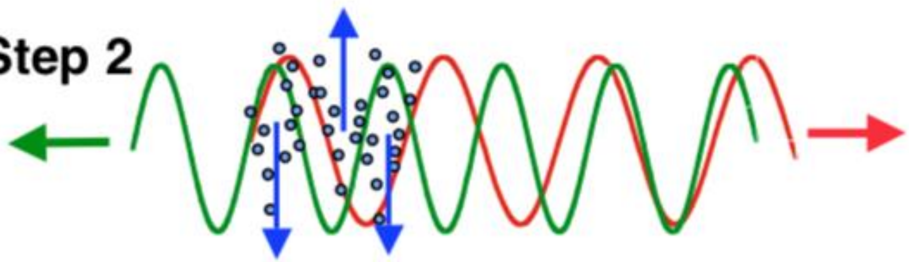

Oscillations in the plasma begin to radiate scattered light

Step 3

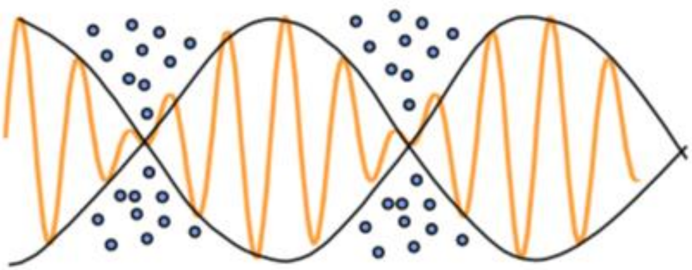

The beating of the two light waves creates a ponderomotive force pushing the particles into the troughs of the envelope

Step 4

Electrostatic plasma wave

If the bunching of the particles matches an electrostatic mode, the 3 waves become resonant and grow

3 wave parametric decay

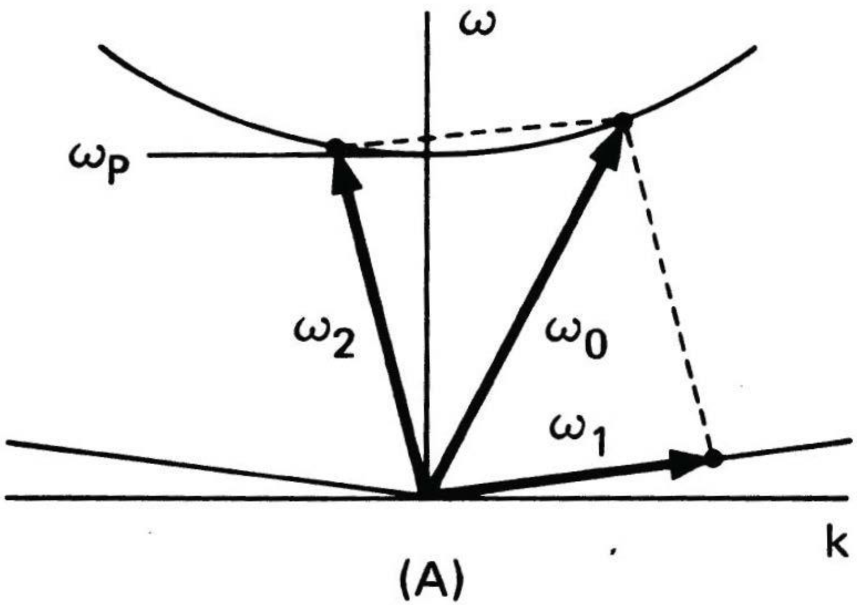

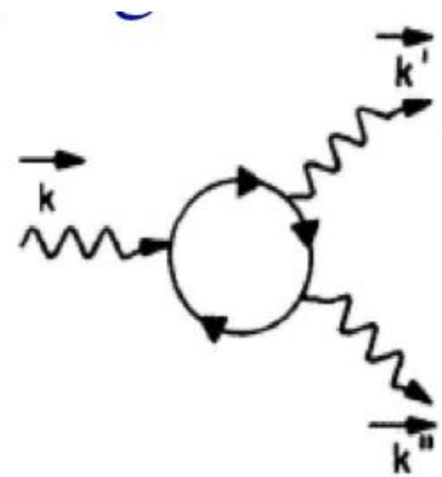

These can be considered as a Feynman diagram with one input wave, a scattering matrix, and two output waves.

The energy and momentum of the decay waves must equal those of the input wave:

$$\omega_0 = \omega_1 + \omega_2$$

$$k_0 = k_1 + k_2$$

since Energy = ħν and momentum P = ħk

arranging: $\omega_0 - \omega_2 = \omega_3$

$$k_0 - k_2 = k_3$$

the frequencies ω_0 and ω_2 are beating and a non-linear interaction element will produce ω_3.

or dividing $(\omega_0 - \omega_2)/(k_0 - k_2) = \omega_3/k_3$

i.e. the group velocity of the high frequency waves must equal the phase velocity of the low frequency wave

For unmagnetised plasmas (or for $\omega_{pe} << \omega_{ce}$) the interaction occurs near the plasma frequency.

$\omega^2=\omega_{pe}^2+3/2\ v_{eth}^2k^2$

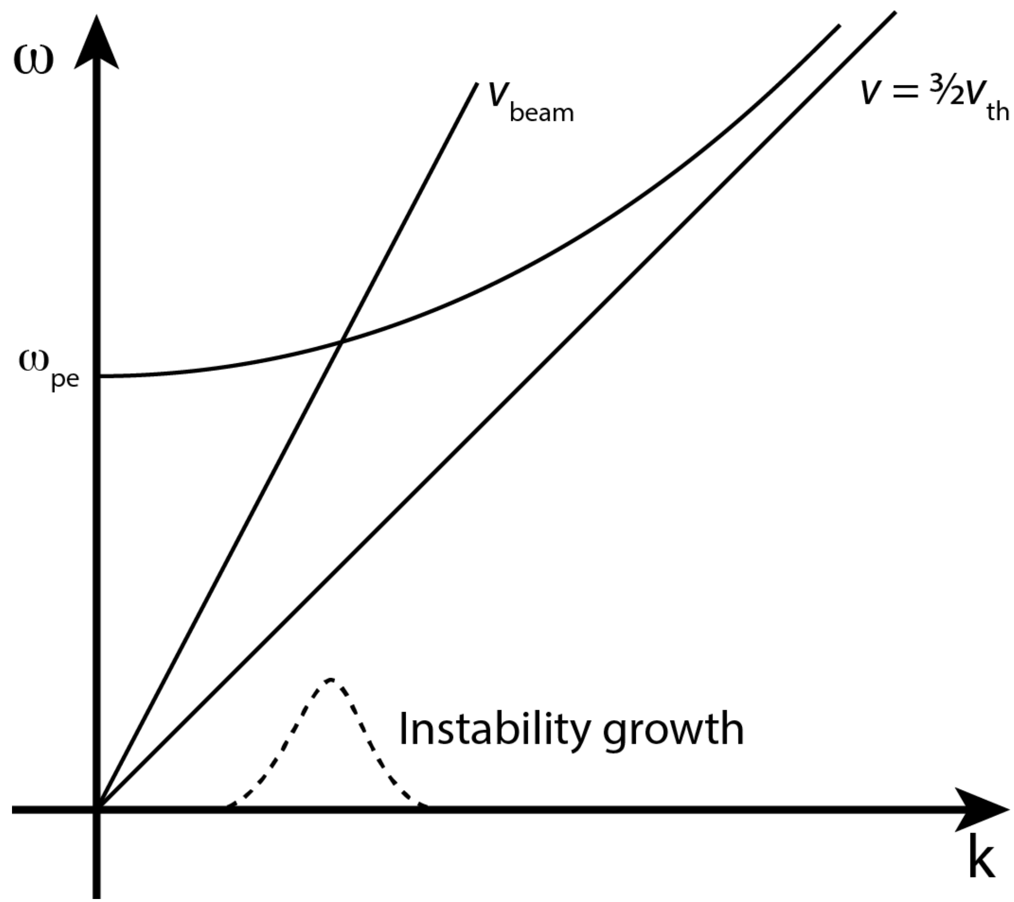

Electron beams support fast and slow waves, propagating with and against the beam direction, these waves interact with the electron plasma (Langmuir) waves to produce instabilities.

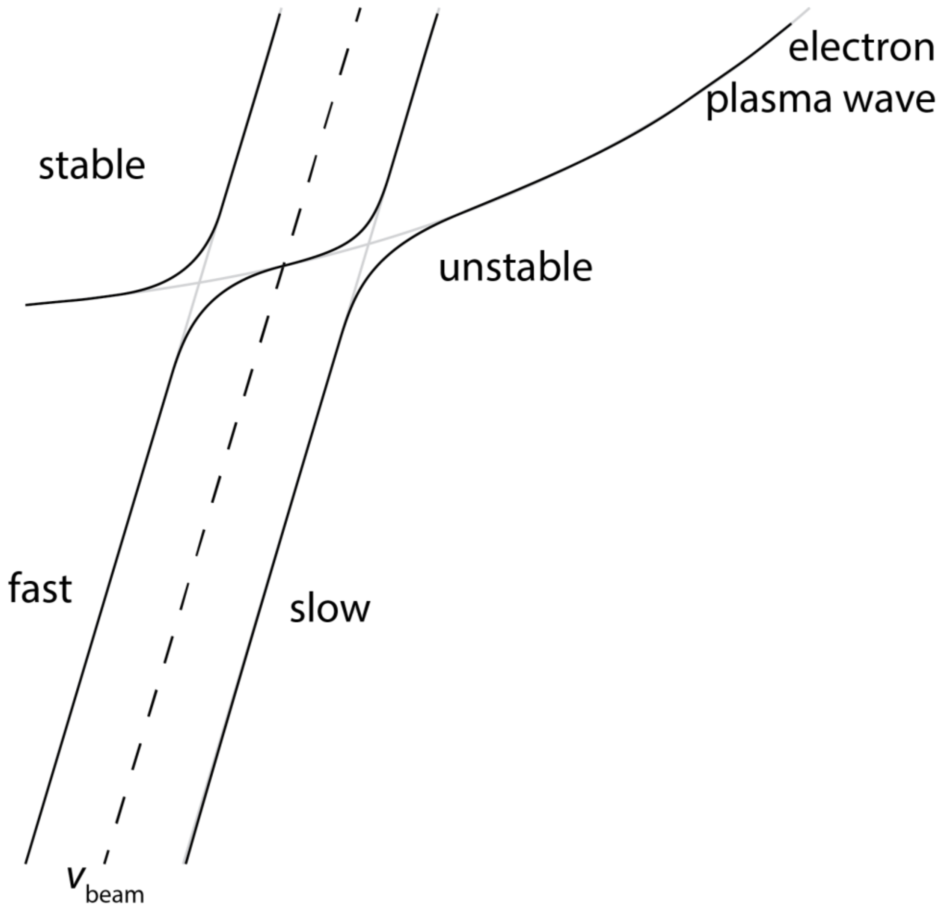

In a magnetised plasma the beam interacts with oblique waves on the upper hybrid and whistler resonance cones

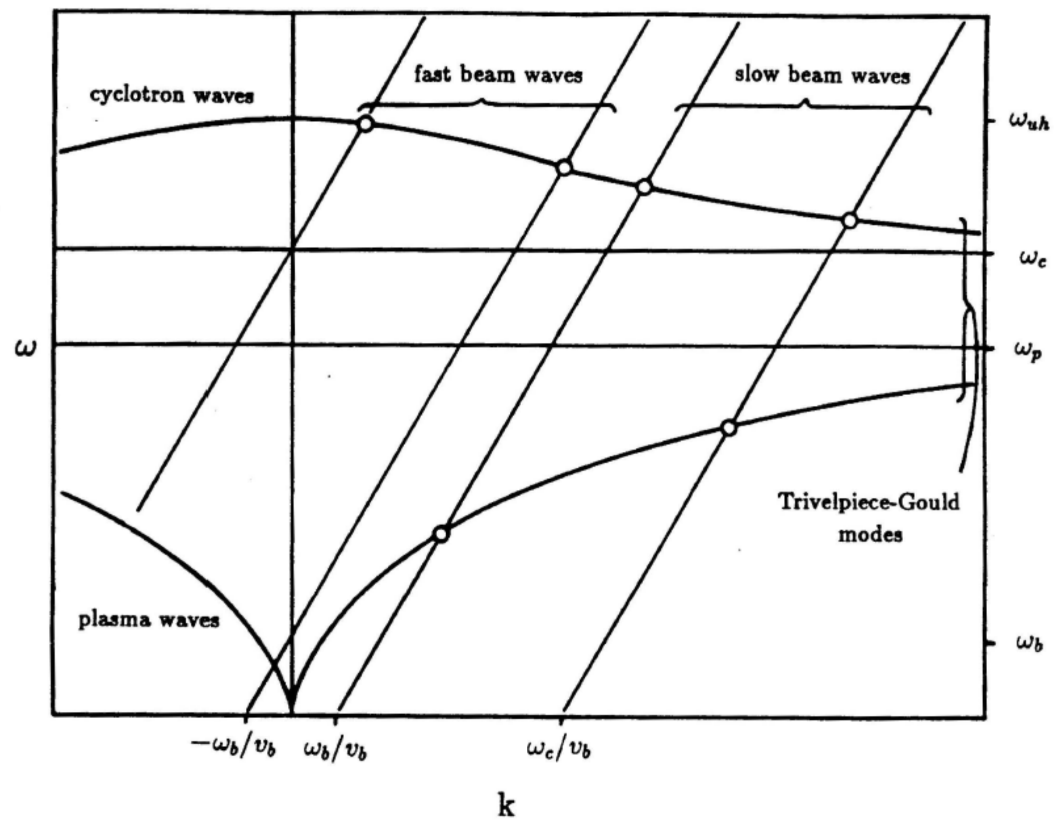

Figure 1.1: *The dispersion relation of Simpson and Dunn (1966) for a beam-plasma interaction in cylindrical geometry. The circles show the regions where the fast and slow beam waves may couple with the Trivelpiece-Gould modes of the plasma.*

Rocket experiments launched electron beams along a field line to the earth’s congugate point, beam plasma discharge postulated to explain rocket neutralisation (and Hall Effect neutraliser used!)

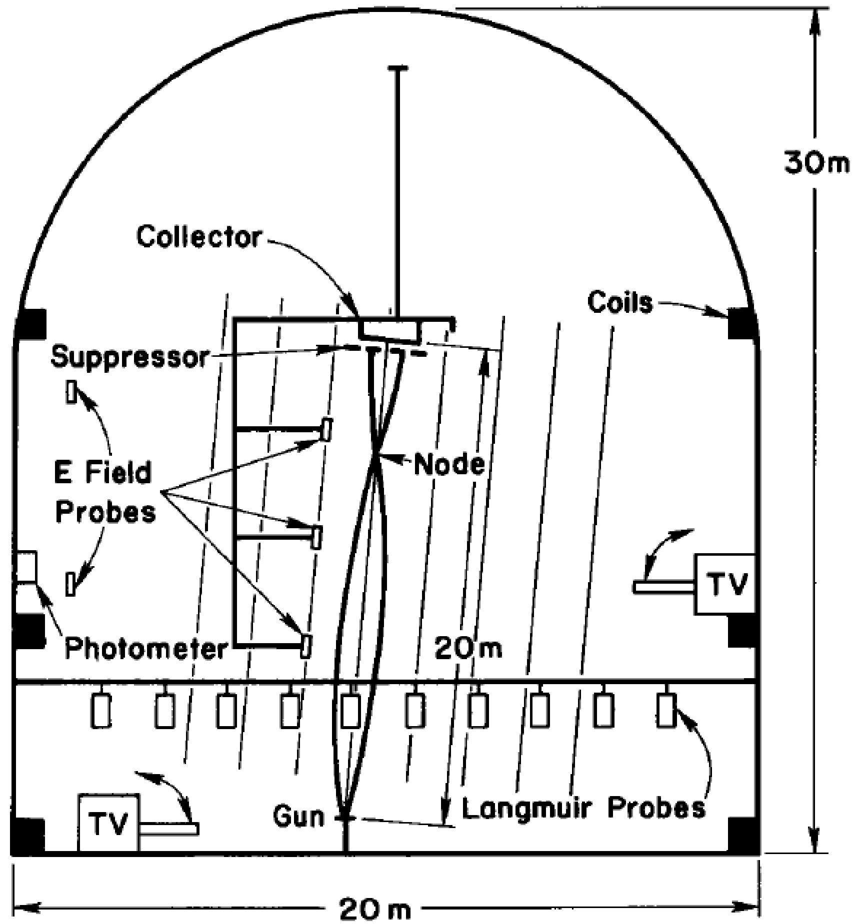

Fig. 1. Schematic representation of the experimental arrangement.

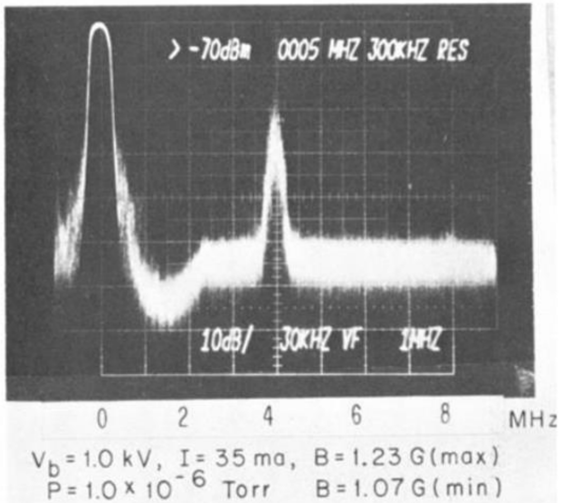

(a) LOW DENSITY

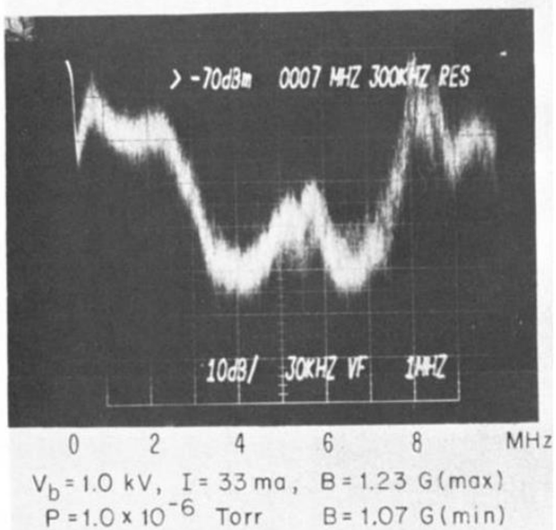

(b) HIGH DENSITY

Bernstein et. al. in 1978 observed two types of BPD, low density ($\omega_{pe} < \omega_{ce}$) and high density ($\omega_{pe} > \omega_{ce}$).

WOMBAT (Waves On Magnetised Beams And Turbulence) was constructed at the ANU to simulate the Space Shuttle environment and active experiments with charged particle beams.

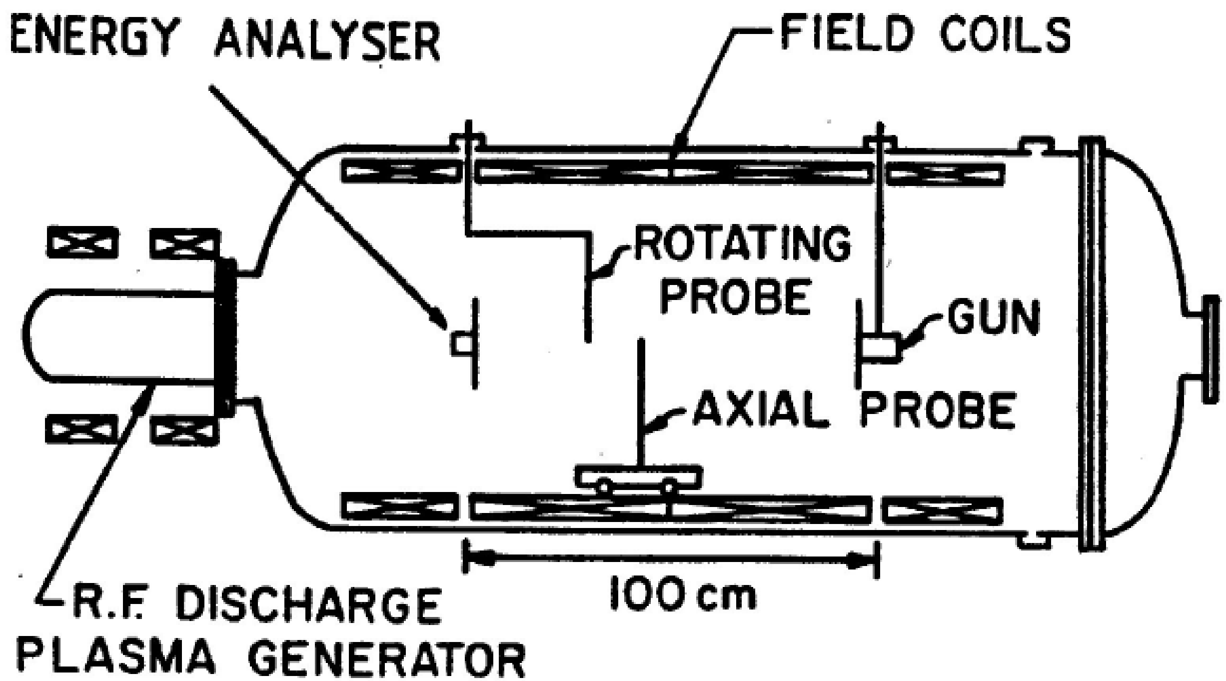

Figure 2.1: *Schematic diagram of the WOMBAT apparatus.*

Four types of BPD were discovered in WOMBAT (f_{ce} = 100MHz)

BPD1 when ($\omega_{pe} < \omega_{ce}$)

BPD2 when ($2\omega_{ce} > \omega_{pe} > \omega_{ce}$)

BPD3 and BPD4 ($\omega_{pe} >> \omega_{ce}$)

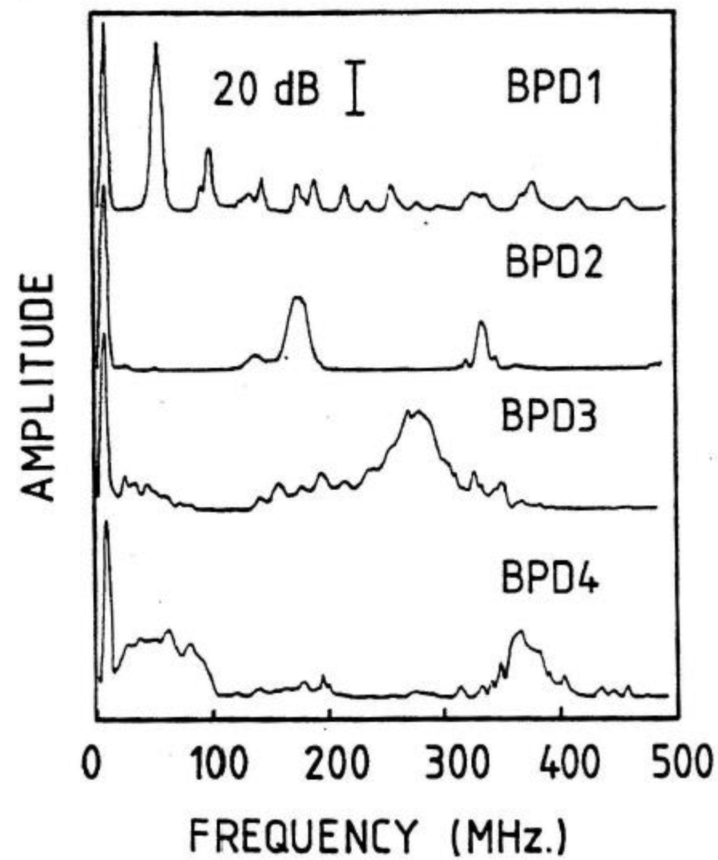

Figure 2.8: *Typical spectra of the first four BPD's, when $\mathcal{E}_b = 300$ eV and $B_0 = 36$ G.*

As the beam current was increased, the frequency of the BPD1 bursts increased and the deduced plasma density increased linearly with beam current (ie. ionisation rate).

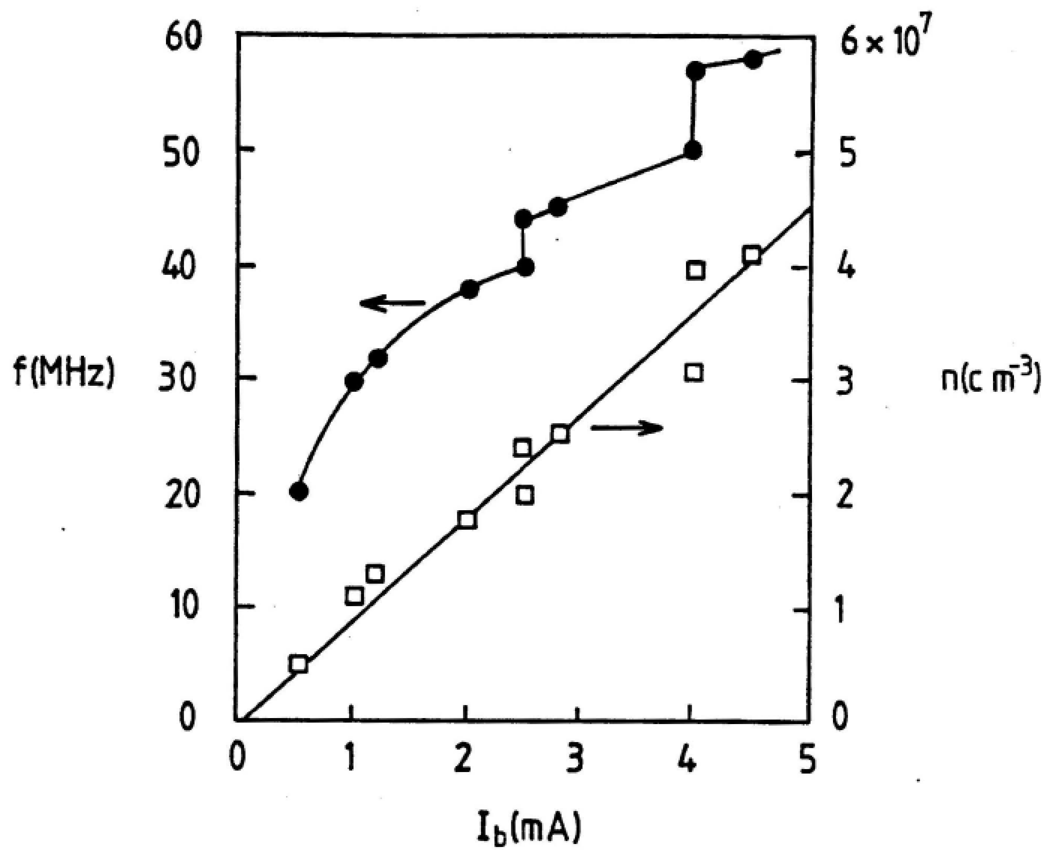

Figure 2.11: *a) Frequency of the BPD1 bursts with increasing I_b. b) Plasma density estimated by assuming that the oscillations are at f_e.*

The bursts grew axially away from the electron gun at a rate approximately ~ $(n_{beam}/n_{plasma})^{1/4}\omega_{pe}$. They were axially modulated by the finite number of wavelengths that could fit in the system (Pierce)

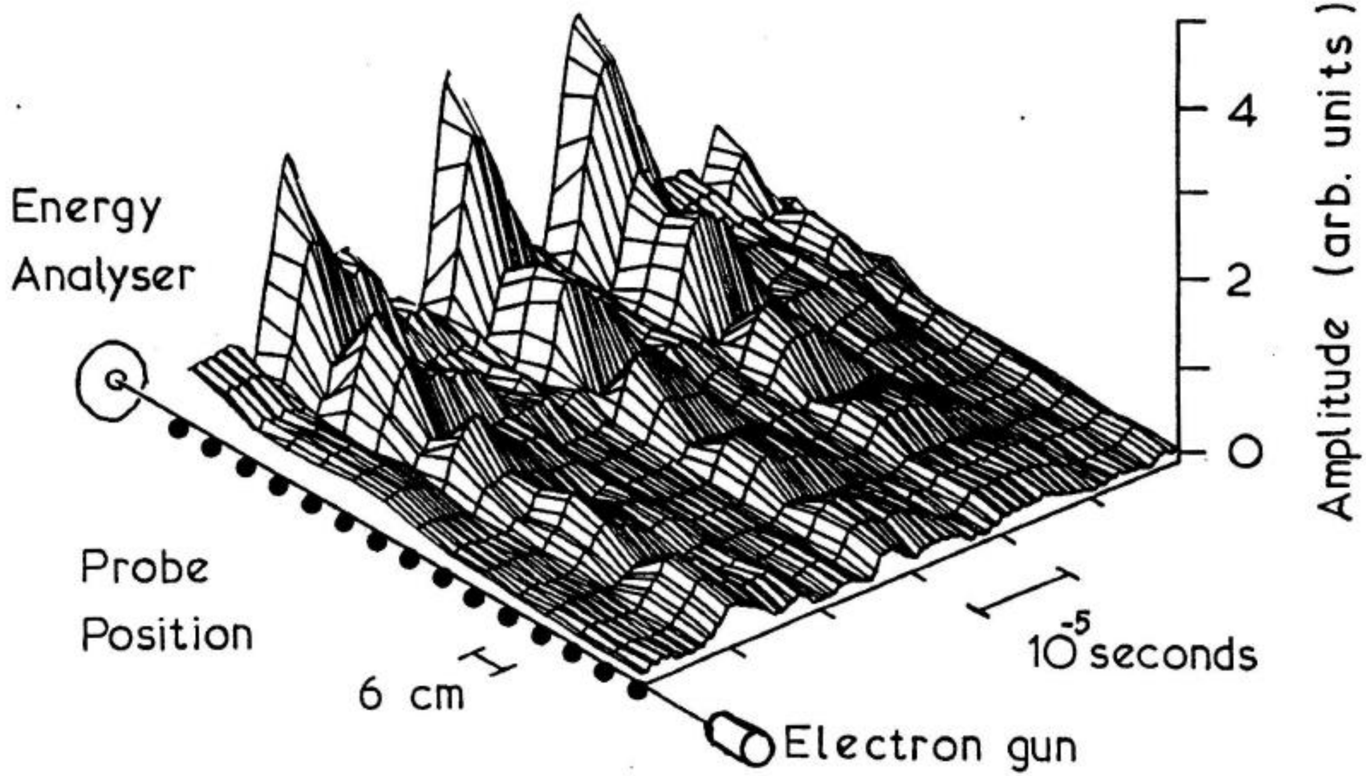

Figure 2.13: *Envelopes of the 30-40 MHz bursts measured with* 16 *probes spaced* 6 *cm apart along the axis of the electron beam.*

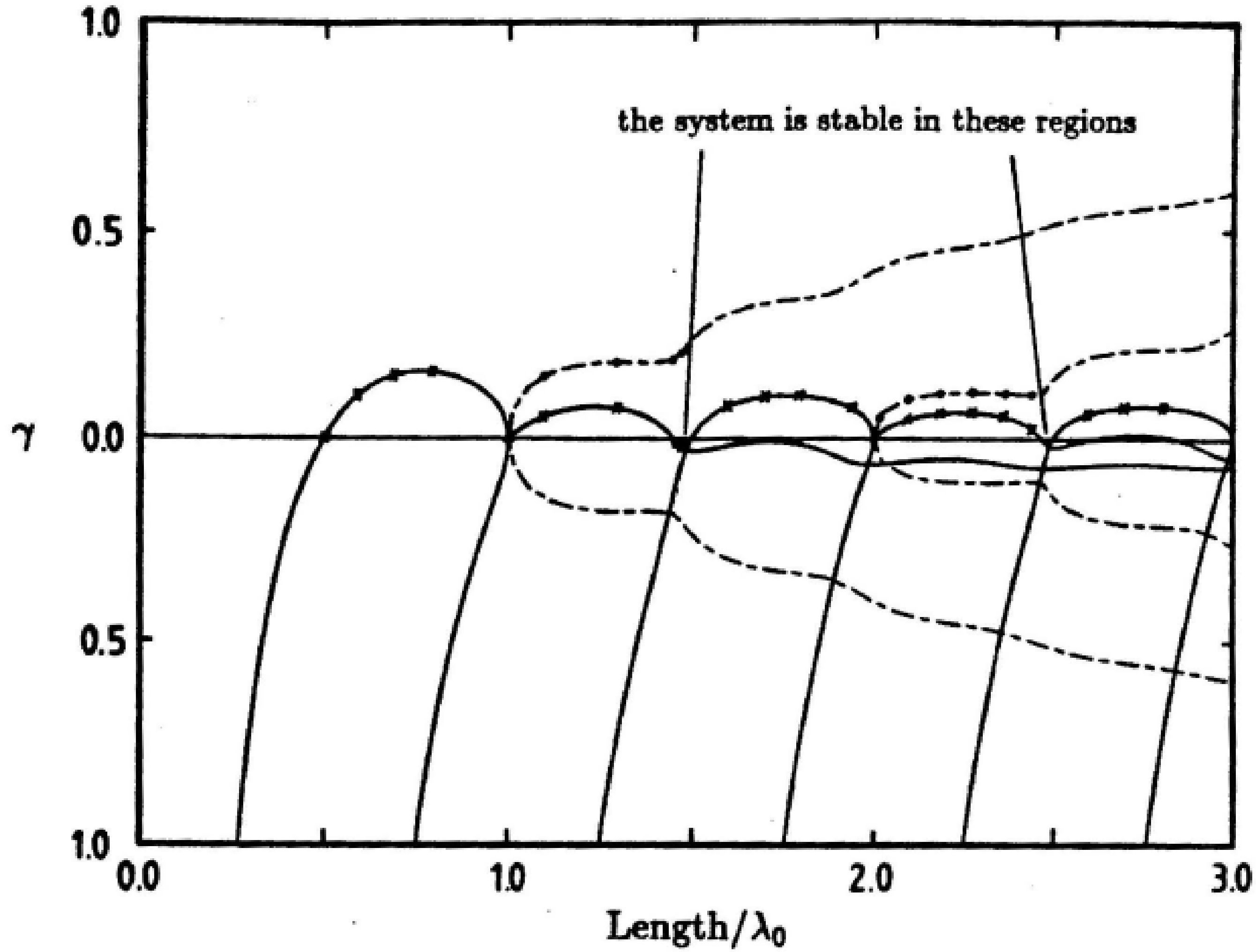

Figure 4.1: *The dispersion relation for the original Pierce instability. The solid lines are the real part of γ, ie. the growth rate, and the broken lines are the imaginary part of γ, ie. the frequency.*

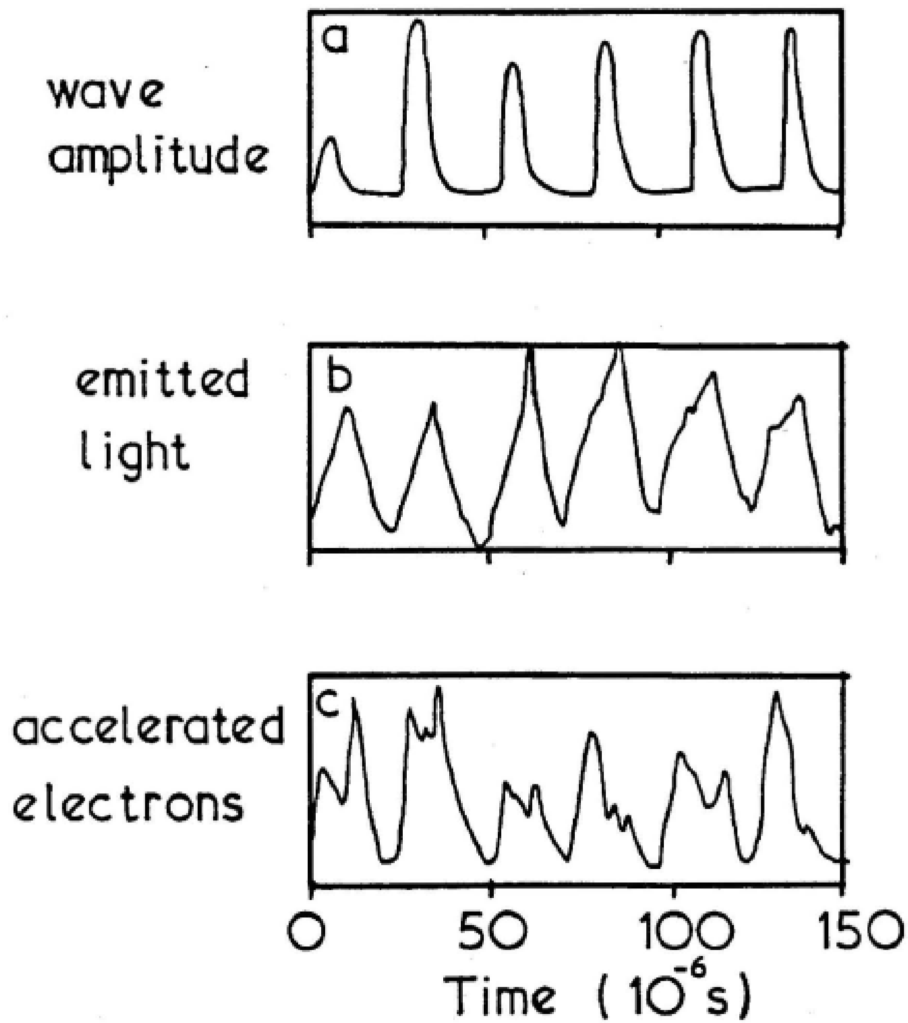

Figure 2.10: *Correlation between a) envelope of the RF burst, b) current to a photomultiplier tube, and c) current reaching the collector of the energy analyser with $V_3 = -15$ volts, for BPD1 bursts.*

For large amplitude bursts, the beam produced waves with sufficient amplitude reverse the motion of the electrons, ie. the beam was stopped by it's own instability!

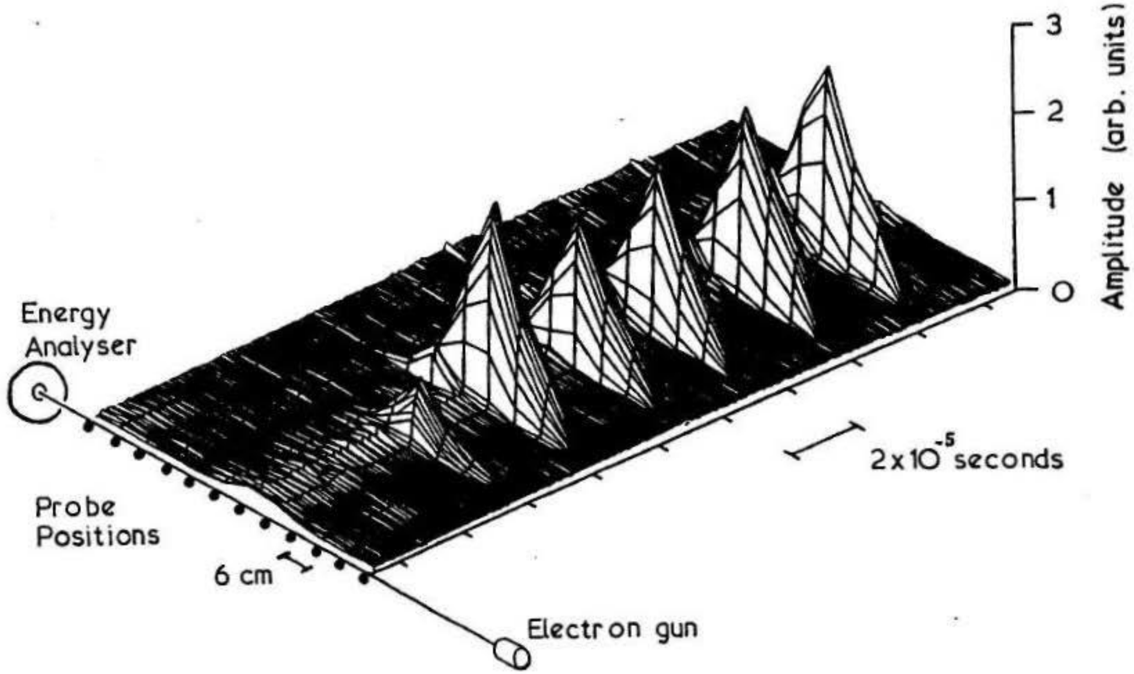

Figure 2.14: *Envelopes of the bursts of about 50 MHz measured with 16 probes spaced 6 cm apart along the axis of the electron beam.*

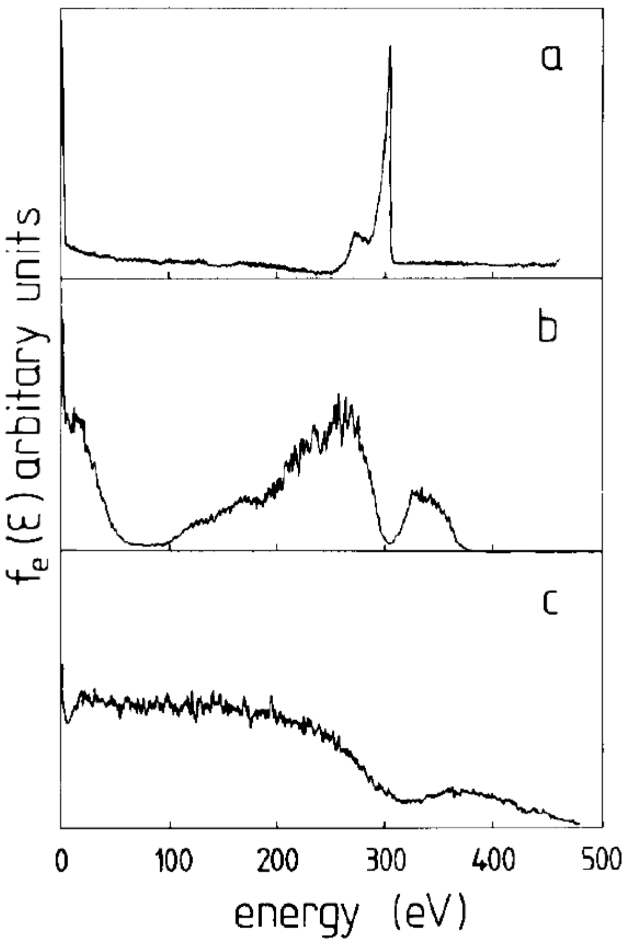

Fig. 2. Electron energy distributions obtained from the differentiated time averaged energy analyzer results, (a) just before BPD, $I_b \sim 3$ mA; (b) just after BPD, $I_b \sim 6$ mA; (c) developed BPD, $I_b \sim 12$ mA. As the potential on the analyser affects the plasma, the beam currents are accurate only to a factor of two.

The electron beam is severely perturbed by the instability, scattering and phase mixing down to lower energies. The additional Beam Plasma Discharge produced an excess of low energy electrons which increase the ionisation rate.

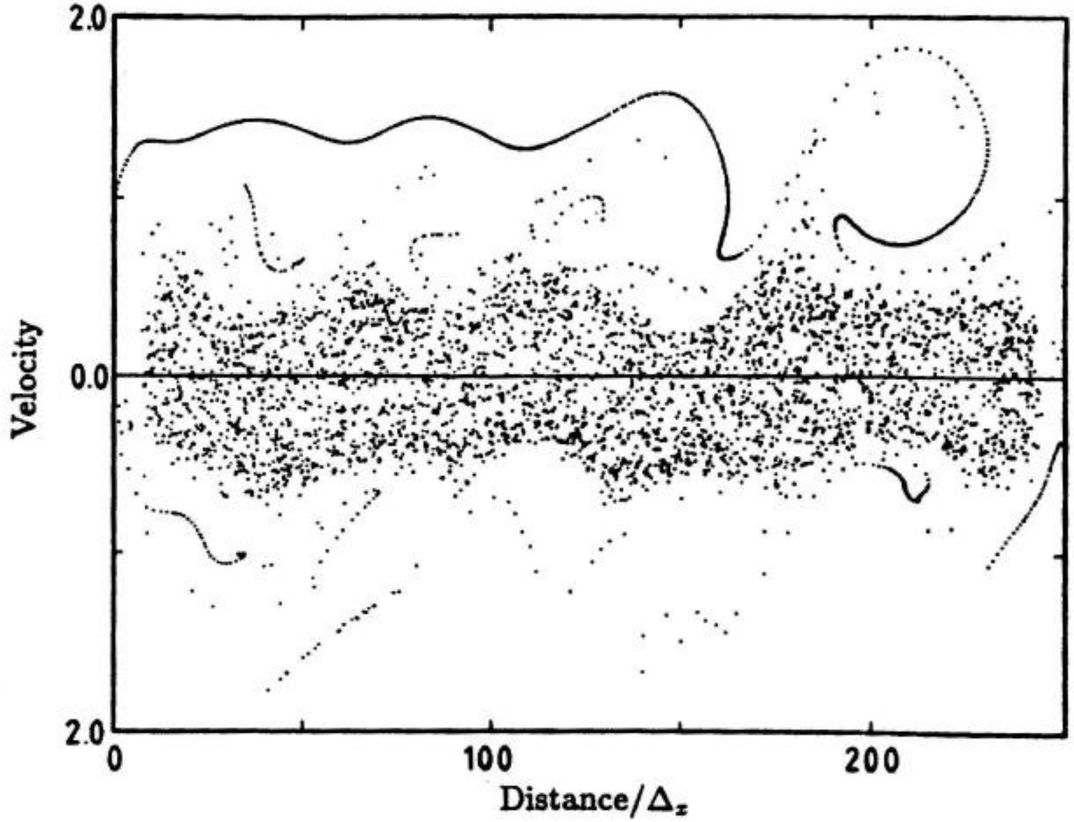

2.0
0.0
2.0
0
100
200
Velocity
Distance/Δ_x

Waves generated by the beam can become sufficiently high to parametrically decay into lower frequency waves.

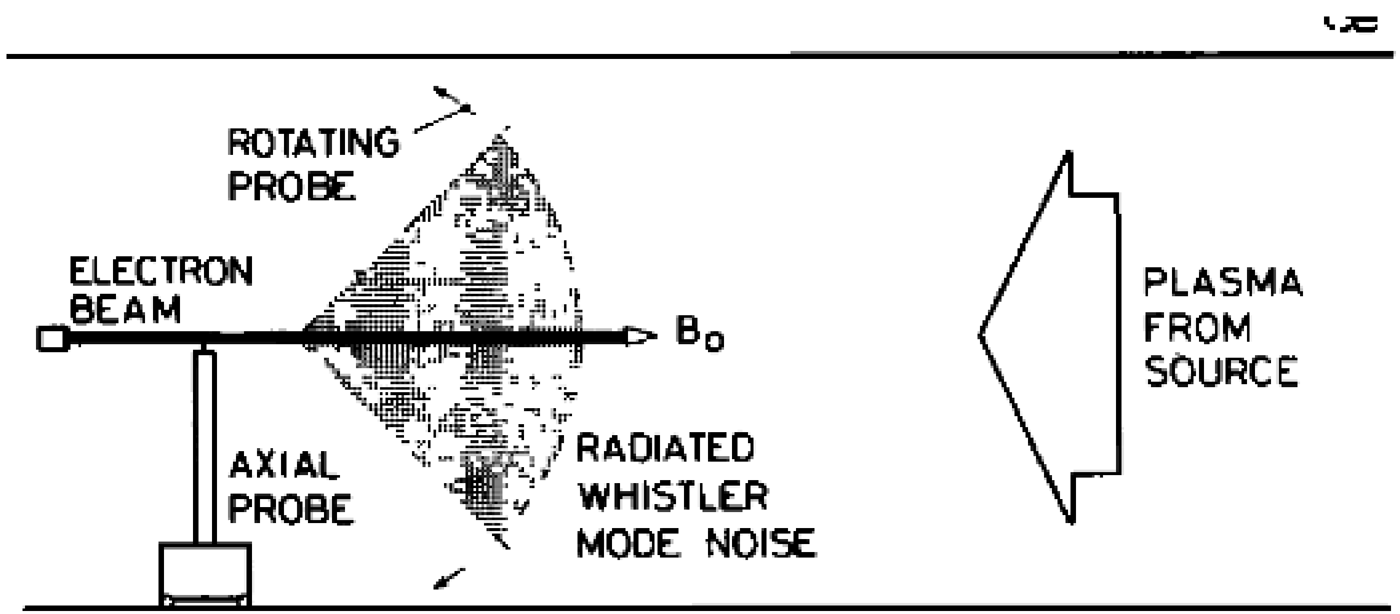

Figure 1. Schematic diagram of the experiment.

In this experiment, the beam convectively excites waves at the upper hybrid frequency (A) which then decay to a non propagating wave at the electron cyclotron frequency and a whistler on the resonance cone (B) and finally to broad band waves by cascading (C). The spatial evolution of the pump, sideband and daughter are shown in (D).

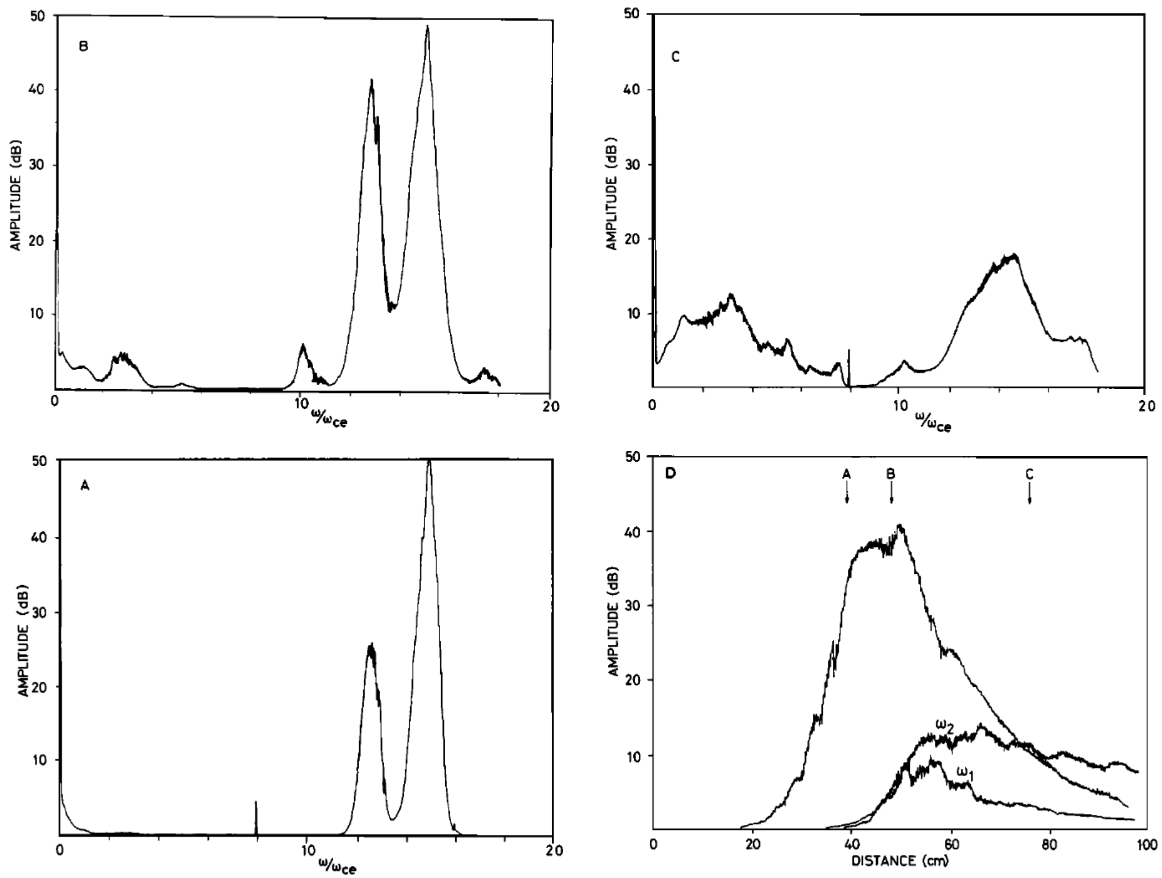

Figure 2. Wave spectra in the beam at 35 cm (a), 50 cm (b), and 75 cm (c) and (d) amplitude as a function of distance from the gun for waves at 1.3, 1.01 and 0.3 ω_{ce}.

References

R.W. Boswell, Non-convective Parametric Instability Associated with Whistler Wave Resonance Cone, *Phys. Lett.* 55A 93-94 (1975).

C.D. Reeve and R.W. Boswell Parametric Decay of Whistlers - A Possible Source of Precursors, *Geophys. Res. Lett.* 3 405-407 (1976).

R.W. Boswell and M.J. Giles, Generation of Whistler Mode Radiation by Parametric Decay of Bernstein Waves, *Phys. Rev. Letts.* 39 277-280 (1977).

R.W. Boswell VLF Hiss Generated by Suprathermal Electrons, Geophys, *Res. Letts.* 3 705-707 (1976).

R.W. Boswell and P.J. Kellogg Characteristics of Two Types of Beam Plasma Discharge in a Laboratory Experiment, *Geophys. Res. Letts.* 10 (7) 565-568, (1983).

R.W. Boswell, S.M. Hamberger, P.J. Kellogg, I.J. Morey and R.K. Porteous Direct observation of rapid impulsive electron heating during a beam plasma interaction, *Phys. Letts.* 101A 501-504 (1984).

R.W. Boswell Experimental Measurements of Bifurcations, Chaos and Three Cycle Behaviour on a Neutralized Electron Beam, *Plasma Physics and Controlled Nuclear Fusion* 27 405-418, (1985).

R.W. Boswell and P.J. Kellogg, Beam Plasma Instabilities and the Beam Plasma Discharge, *Phys. Fluids* 29 1669-1674 (1986).

R.W. Boswell, I.J. Morey and R. K. Porteous, Wave Phenomena Preceding and During a Beam Plasma Discharge, *Journal of Geophysical Research* 94A3, pp2654-2666 (1989).

I.J. Morey and R.W. Boswell Evolution of Bounded Beam-Plasma Interactions in a one-dimensional particle simulation, *Phys Fluids B, Plasma Phys* 1 (7) 1502-10 (1989).

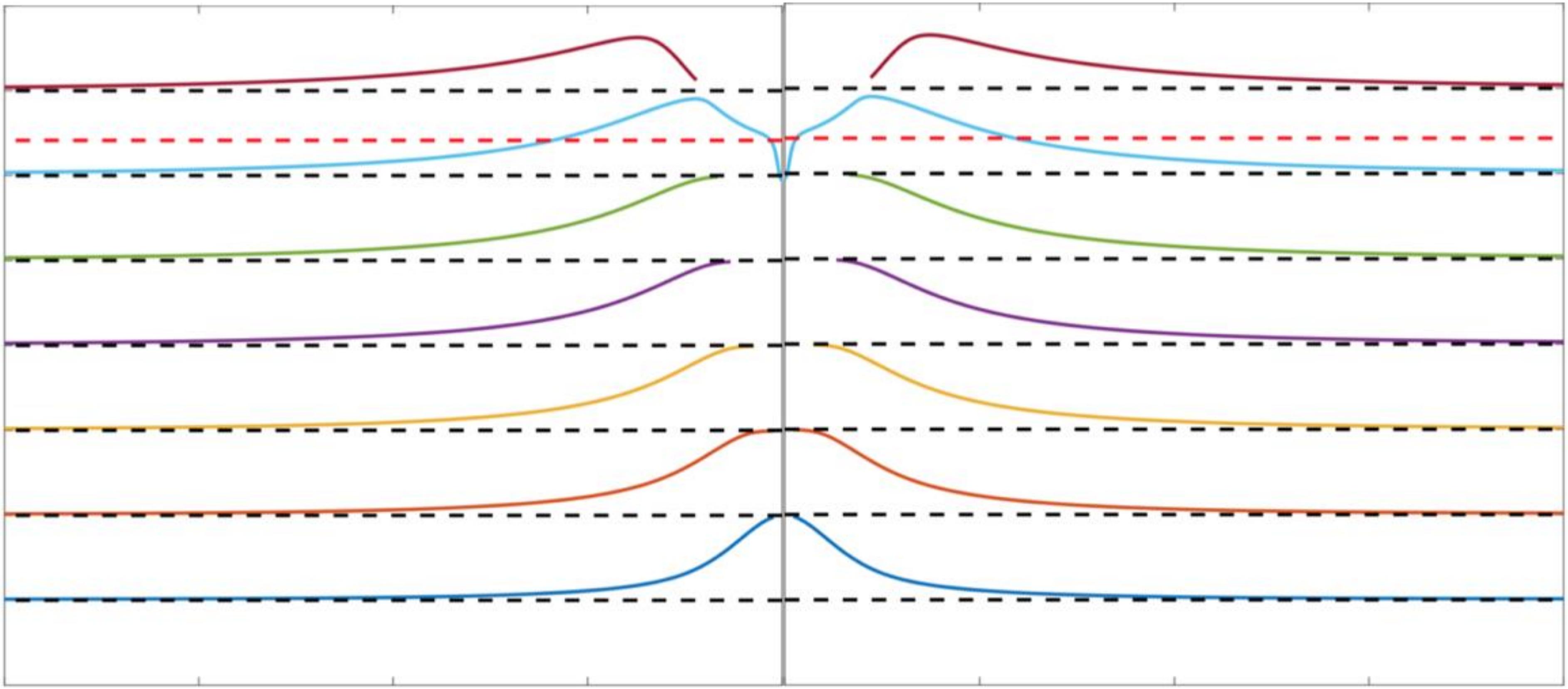

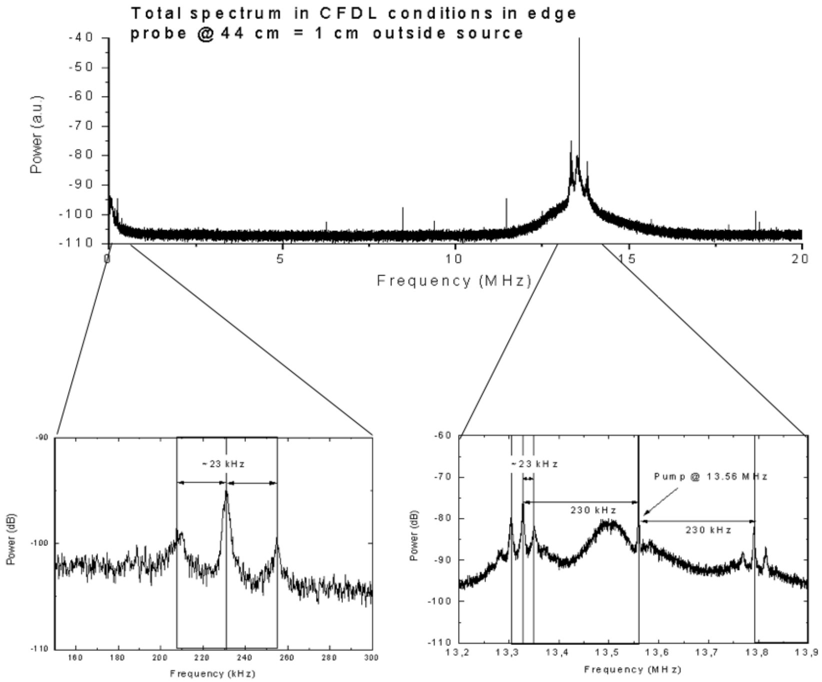

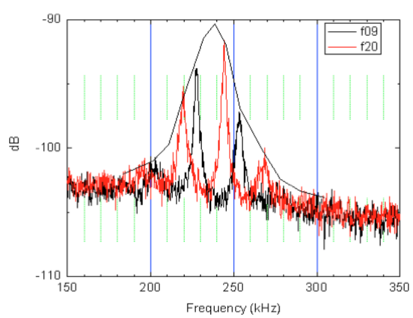

Figure 8. The base group of lines shown in high resolution. Spectra at high pressure (red, p= 0.78 mTorr) and low pressure (black, p=0.42 mTorr) are superimposed to illustrate the line shifts.

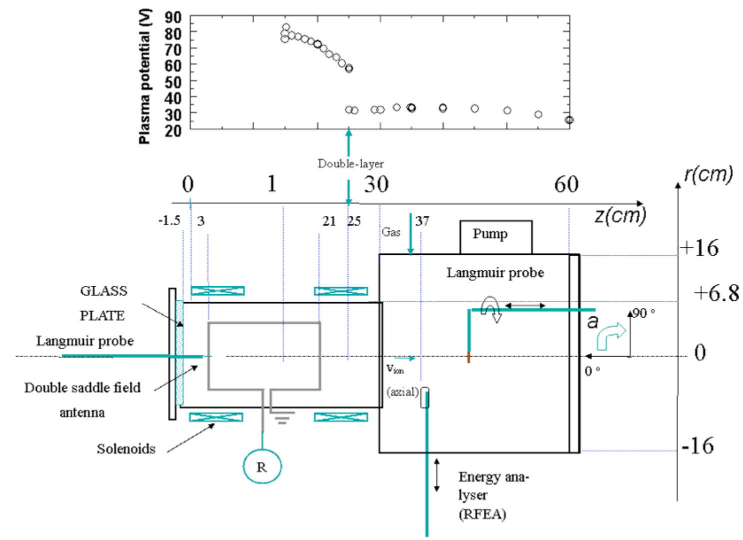

Figure 1

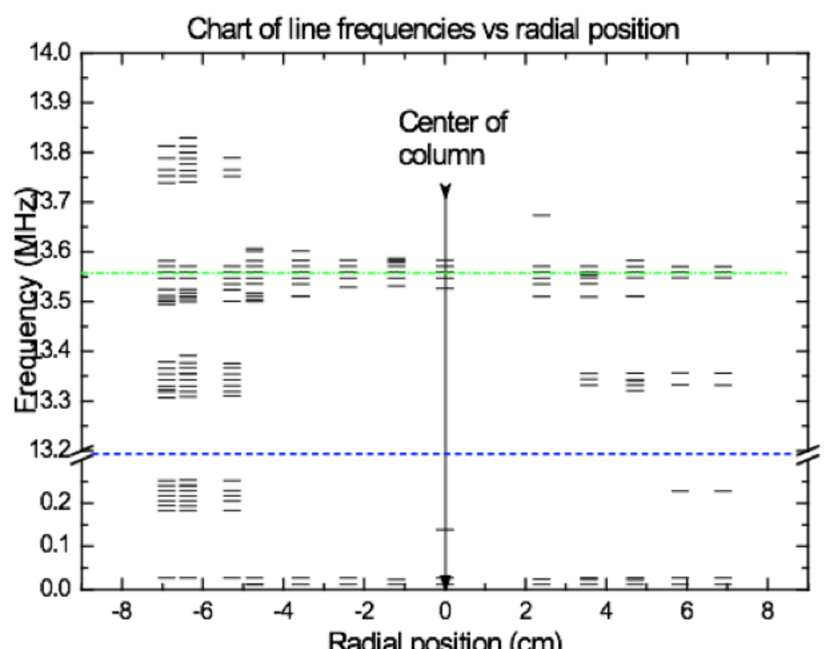

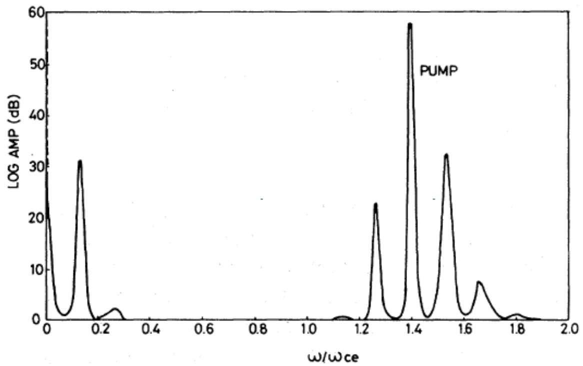

FIG. 1. Decay spectrum near the transmitting anten-

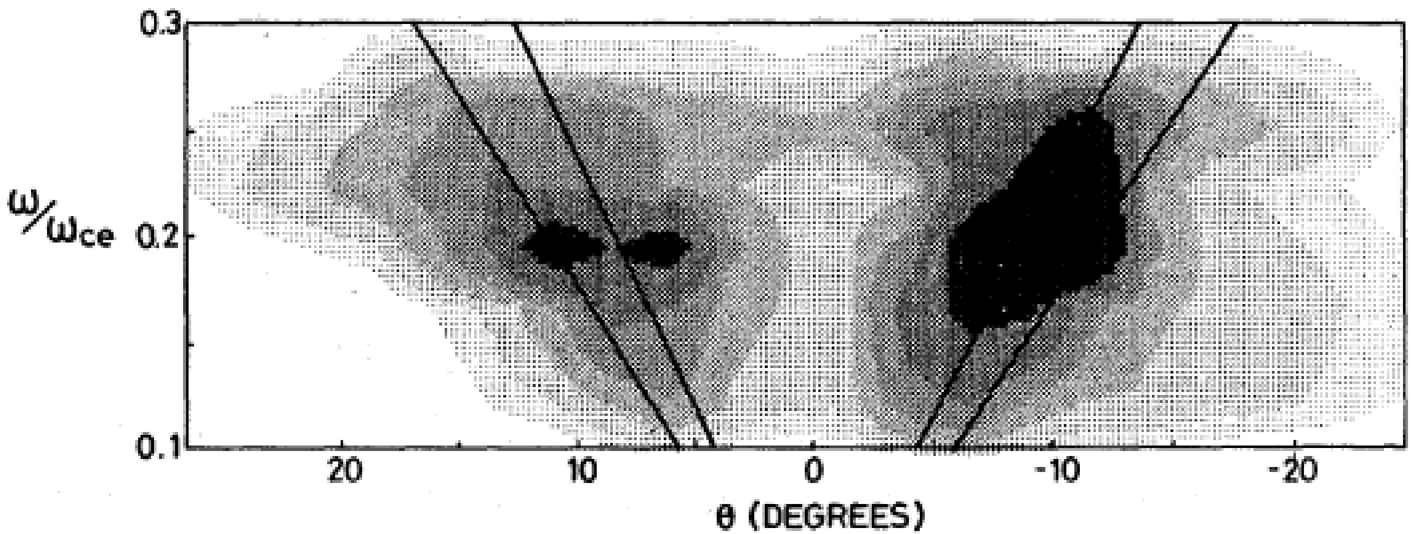

FIG. 2. Low-frequency spectrum as a function of angle to $\vec{B}_0$ for 30 W input power. The eight grey shades represent an amplitude range of 20 dB.

Instabilities in Vasimr

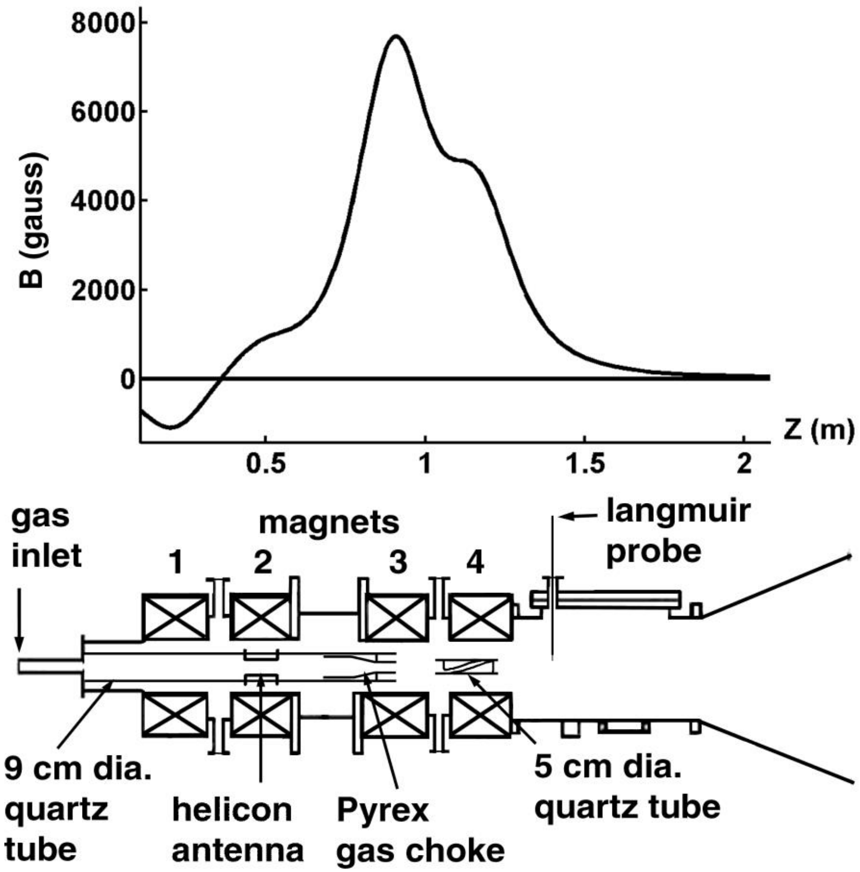

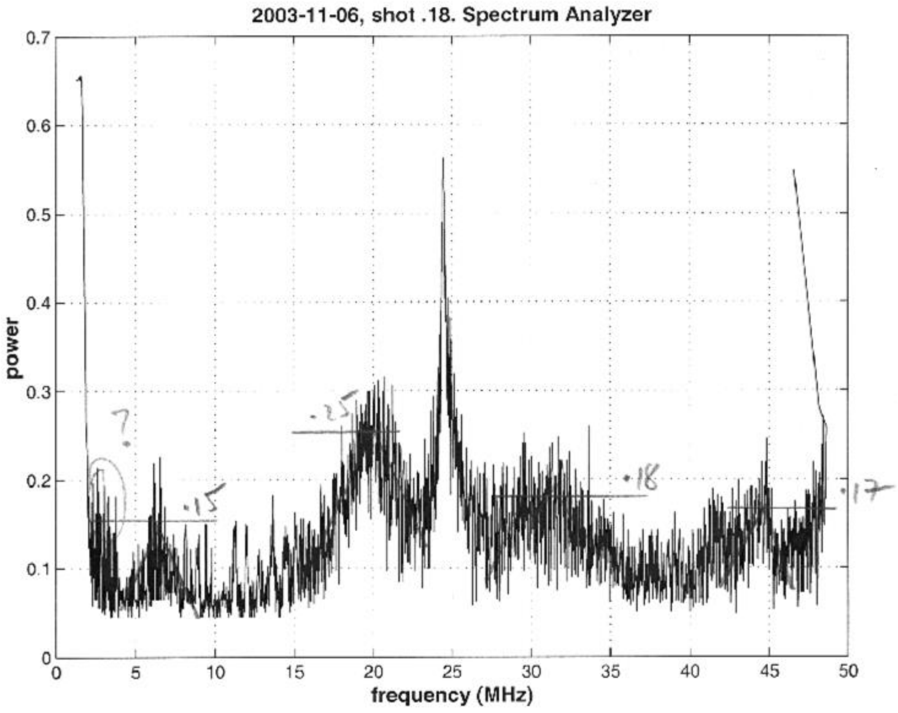

simple helicon dispersion $\lambda \sim 5 \times 10^9 (B/fn)^{1/2}$

Assuming that $n \sim 10^{13}$ cm^{-3} and $B \sim 700$ Gauss, conditions typical near the helicon source:

For the 25 MHz pump	$\lambda \sim 8.5$ cm	$k \sim 0.74$
For the 20 MHz daughter	$\lambda \sim 9.5$ cm.	$k \sim 0.66$
For the 5 MHz idler	$\lambda \sim 19$ cm	$k \sim 0.33$

Wave Amplitude vs. Position

Wave Amplitude vs. Position